Scripta Materialia xxx (2015) xxx–xxx

Contents lists available at ScienceDirect

Scripta Materialia

journal homepage: www.elsevier.com/locate/scriptamat

Transient liquid-phase bonded 3D woven Ni-based superalloys

Dinc Erdeniz [a,*], Keith W. Sharp [b], David C. Dunand [a]

[a] Department of Materials Science and Engineering, Northwestern University, 2220 Campus Drive, Evanston, IL 60208, USA
[b] SAERTEX USA, LLC, 2200-A Mt. Holly-Huntersville Road, Huntersville, NC 28078, USA

ARTICLE INFO

Article history:
Received 26 March 2015
Revised 2 June 2015
Accepted 13 June 2015
Available online xxxx

Keywords:
Nickel alloys
Pack cementation
Liquid-phase sintering
Microstructure
Mechanical properties

ABSTRACT

Architectured Ni-based superalloy scaffolds were fabricated by three-dimensional weaving of ductile Ni–20Cr (wt.%) wires followed by gas-phase alloying with aluminum and titanium via pack cementation. Bonding of neighboring wires occurs at necks that are formed by solid-state diffusion or by formation of a transient-liquid phase. Three-point bending tests of the superalloy weaves, after homogenization and aging to achieve a γ/γ' structure, show that, as bonding between wires increases, the materials withstand higher stresses and strains before onset of damage.

Architectured cellular materials [1–8], such as honeycombs [4], trusses [5], and wire-based structures [6–8], offer a combination of low density and high specific strength, stiffness, permeability, and surface area. These materials have periodic structures that can be designed by using topological optimization models to enhance the desired properties [9–11]. One example is 3D woven metal structures, fabricated from Cu or Ni–Cr wires, that are topologically optimized to provide improved permeability in preferred directions with minimal loss in stiffness for thermo-structural applications [8]. Such cellular materials are of interest for extreme environments, since increased permeability allows for active cooling and results in prolonged service life, or even enables material use, at elevated service temperatures and stresses. A number of studies have been published in the area of periodic cellular nickel-based superalloys, none, however, using topological optimization tools [12–14]. The main reason for the limited number of existing studies is the difficulty in the processing of such superalloy architectured structures. Particularly, processing of wire-based structures are very challenging due to three manufacturing obstacles: (i) superalloy wires, especially below 500 μm diameter, are difficult to draw, and hence not widely available through suppliers, (ii) if drawn, they are not sufficiently ductile to withstand the bending angles required for weaving, and (iii) if woven, the contact points must be bonded to reach the full potential of mechanical properties, which is difficult due to the presence of oxide layers at the wire surface and low diffusivity, limiting the extent of solid-state bonding.

In a recent study, we reported the fabrication of topologically optimized Ni–Cr–Al superalloy structures produced using 3D textile processes [7,8]. Ni–20Cr (all compositions are given in wt.% hereafter) wires were 3D woven or 3D braided, taking advantage of the room-temperature ductility of these wires, and subsequently aluminized via pack cementation [7], a chemical vapor deposition process that has been widely used to create aluminide coatings on Ni-based superalloys for corrosion protection [15–17]. Aluminized 3D woven structures were then homogenized into Ni–Cr–Al alloys and aged for the precipitation of γ' particles, which are responsible for the high temperature creep resistance of superalloys. Simultaneously, the Ni–Cr–Al wires bonded by solid-state diffusion at their contact points during pack aluminization and homogenization [7]. In the present study, we demonstrate that Al and Ti can be co-deposited by pack cementation onto woven Ni–20Cr structures, which are then homogenized and aged to create Ni–Cr–Al–Ti superalloys where both Al and Ti act as γ' formers. We further show the bonding of the wires via the formation of a transient-liquid phase (TLP) due to the presence of Ti and evaluate the bending properties of the bonded and non-bonded structures.

Materials used in this study are non-crimp 3D orthogonal woven structures fabricated from soft-annealed Chromel A wires (Ni–20Cr–1Si–0.05Fe, labeled Ni–20Cr in the following) with a diameter of 202 μm (32 gauge). A detailed description of the weaving process is given in Ref. [7] and the particular architecture used in the present work is labeled as "optimized weave," in which

* Corresponding author at: 2220 Campus Drive, Cook Hall 2036, Northwestern University, Evanston, IL 60208, USA.
E-mail address: d-erdeniz@northwestern.edu (D. Erdeniz).

http://dx.doi.org/10.1016/j.scriptamat.2015.06.016
1359-6462/

topological optimization selected wire positions that are left vacant to increase material permeability. Woven samples, cut to a length of 72 mm, a width of 12 mm, and a thickness of 3.5 mm (corresponding to 11 wire layers), were buried in a pack mixture consisting of 57 wt.% Al_2O_3 powders (20–50 μm particle size) as filler, 30 wt.% Ti powders (99.5% purity, −325 mesh) and 10 wt.% Raney Ni precursor powders (Ni–50 wt.% Al, 150 μm particle size) as sources, and 3 wt.% NH_4Cl powders (100 μm particle size) as activator, with all powders procured from Alfa Aesar. At elevated temperature, the activator decomposes and reacts with the source powders to create a mixture of titanium and aluminum chloride gas, which subsequently deposits the metallic atoms onto the substrate [18,19]. Approximately 40 g of pack was poured in a steel retort, where the internal pressure rises at elevated temperatures, and the cut specimen was placed at the center of the retort. The inner wall of the steel retort was spray-coated with boron nitride to minimize contamination. The retort was placed at the water-cooled end of a tube furnace that was heated to 1000 °C. After flushing the furnace tube with Ar for 15 min, the retort was pushed into the hot zone of the furnace, where it was held for 30 or 60 min. The retort was then pulled back to the water-cooled end of the tube and cooled there for 15 min. The specimens were removed from the pack and ultrasonicated in acetone for 2 h to remove all pack remnants. Samples cut from each specimen were vacuum-encapsulated in quartz tubes and heat-treated for homogenizing (1100–1200 °C, 48 h), solutionizing (1200 °C, 2 h), and aging (900 °C, 12 h). All heat-treatments were terminated with water quenching.

Samples were mounted in epoxy and prepared via standard metallographic techniques. An etchant composed of 33 vol.% deionized water, 33 vol.% acetic acid, 33 vol.% nitric acid, and 1 vol.% hydrofluoric acid was used to reveal the γ' precipitates. Microstructural and chemical analyses were conducted with an optical microscope and a scanning electron microscope (SEM) equipped with an energy dispersive X-ray spectrometer (EDS). Flexural behavior of the aged samples was evaluated via three-point bending tests with a 50 mm span, following ASTM-D970 and using a crosshead speed of 5 mm/min.

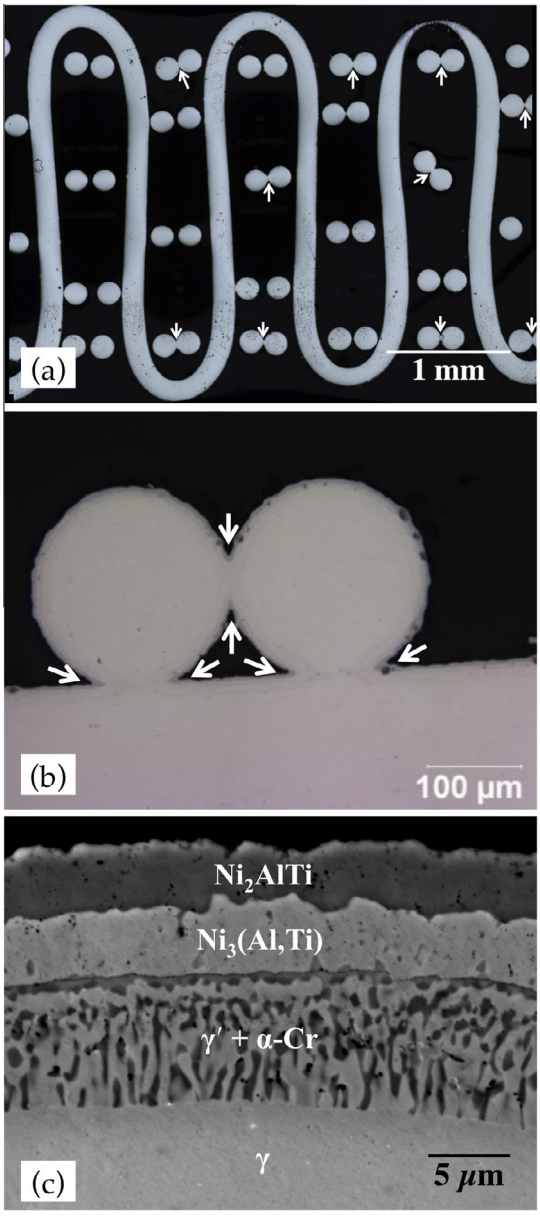

Fig. 1. (a) Optical micrograph showing polished cross-section of Ni–20Cr woven structure alumino-titanized at 1000 °C for 60 min with a total Al + Ti gain of 6 wt.%. Arrows mark the solid-state necks between the wires. (b) Optical micrograph showing a higher magnification image of solid-state bonded necks, where sharp cusps are visible (arrows). (c) SEM image showing the structure of the coating consisting of three layers: outer – Ni_2AlTi, intermediate – $Ni_3(Al,Ti)$, and inner – Cr-rejection in γ' matrix.

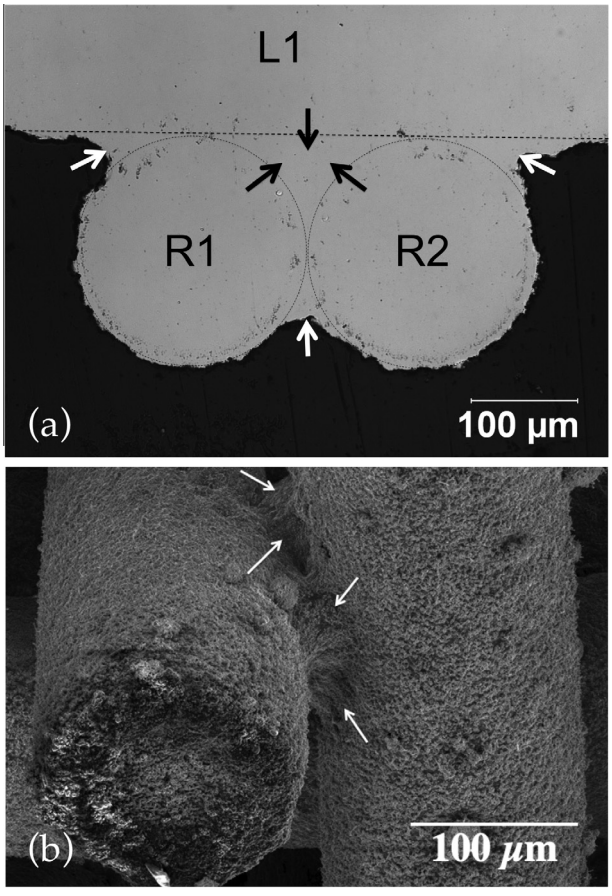

Fig. 2. (a) Optical micrograph showing cross-section of three wires (two radial labeled R1 and R2, one longitudinal labeled L1) which were TLP-bonded together in a Ni–20Cr weave that was alumino-titanized at 1000 °C for 30 min and homogenized/TLP-bonded at 1200 °C for 48 h. The outline of the original wires is shown with dotted lines, and the solidified liquid phase in the necks is marked with arrows. (b) SEM image of the same sample showing necks, marked with arrows, between two orthogonal wires.

Please cite this article in press as: D. Erdeniz et al., Scripta Mater. (2015), http://dx.doi.org/10.1016/j.scriptamat.2015.06.016